Computer Aided Geometric Design 27 (2010) 150–161

Contents lists available at ScienceDirect

Computer Aided Geometric Design

www.elsevier.com/locate/cagd

An intuitive explanation of third-order surface behavior

Pushkar Joshi [a,b,*], Carlo Séquin [a]

[a] University of California, Berkeley, United States
[b] Adobe Systems Inc., United States

ARTICLE INFO

Article history:
Received 29 November 2008
Received in revised form 9 October 2009
Accepted 13 November 2009
Available online 17 November 2009

Keywords:
Third-order shape analysis
Surface interrogation
Curvature derivative
Higher-order surface behavior

ABSTRACT

We present a novel parameterization-independent exposition of the third-order geometric behavior of a surface point. Unlike existing algebraic expositions, our work produces an intuitive explanation of third-order shape, analogous to the principal curvatures and directions that describe second-order shape. We extract four parameters that provide a quick and concise understanding of the third-order surface behavior at any given point. Our shape parameters are useful for easily characterizing different third-order surface shapes without having to use tensor algebra. Our approach generalizes to higher orders, allowing us to extract similarly intuitive parameters that fully describe fourth- and higher-order surface behavior.

1. Introduction

Surface analysis (also known as shape interrogation) is a useful tool for understanding the geometric behavior of a surface near a given point. In the general case of a smooth surface, one can analyze its geometry up to a given order by performing a Taylor expansion of the surface. As an example, the 0th-order surface analysis near a given point yields the position of that point. The first-order analysis adds the tangent plane, the second-order the curvature tensor, and the third-order a rank-3 tensor that describes the derivatives of curvature. The higher the order of surface analysis, the more information about the shape is extracted.

Surface analysis using Taylor expansion produces shape information that is compactly stored in tensors. To extract this information from the tensors, we must formulate an input query in the tensor's coordinate system. For instance, consider the second-order curvature tensor. The curvature tensor is a rank-2 tensor, which means it takes two vectors as input and produces the normal curvature in the direction specified by the vectors. To compute the normal curvature in a given direction at a surface point, we first express the direction as a vector in the point's tangent plane, provide the same vector as both inputs to the curvature tensor, and re-scale the result by the area metric (multiply by the inverse of the first fundamental form). We perform a similarly complicated sequence of operations to extract derivatives of surface curvature; we need to provide three directions to the rank-3 tensor that encapsulates the curvature derivative information. Extracting precise shape information at a surface point thus requires us to understand how to query the shape tensors at that point.

However, most people, especially novices to linear algebra, are more apt to extract shape information from simple geometric primitives. For instance, up to second order we can easily classify a surface point as flat, elliptic, hyperbolic, or parabolic (Fig. 1). We can extract the principal curvatures κ_1 and κ_2 (maximum and minimum values of the normal curvatures at the surface point) from the curvature tensor, and use just those two scalar values to intuitively classify the

* Corresponding author at: Adobe Systems Inc., 345 Park Avenue, San Jose, CA 95110, United States.
E-mail addresses: pushkarj@adobe.com (P. Joshi), sequin@cs.berkeley.edu (C. Séquin).

0167-8396/$ – see front matter
doi:10.1016/j.cagd.2009.11.003

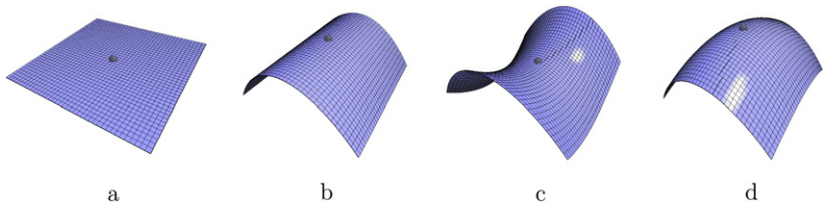

Fig. 1. Up to second order, we can intuitively classify a surface point as (a) flat, (b) parabolic, (c) hyperbolic, and (d) elliptic.

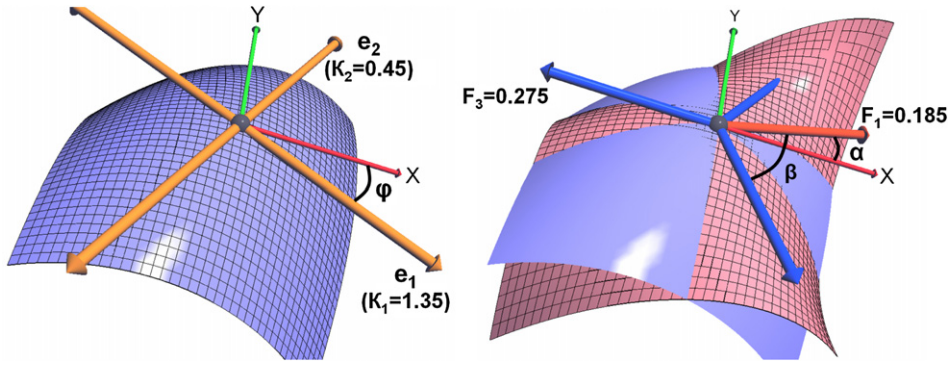

Fig. 2. The above figures show the parameters that fully describe the second-order (left) and third-order (right) shape behavior. All vectors are in the tangent plane of the point of analysis and are unit vectors. *Left*: Second-order frame comprised of principal directions and their associated principal curvatures. The angle ϕ indicates the rotation of the frame from the user provided x-axis in the tangent plane. The entire second-order behavior is described by three numbers: κ_1, κ_2 and ϕ. *Right*: Third-order frame comprised of four directions: one indicating the peak of the first Fourier component and the other three indicating equally spaced peaks of the third Fourier component. Angle α indicates the rotation of the frame from the user provided x-axis, and angle β indicates the rotation of the third Fourier component from the first Fourier component. The entire third-order behavior is described by four numbers: F_1, F_3, α and β. The cubic surface in pink (with the grid) is superimposed on the original quadratic surface in blue (without the grid) to show the undulatory third-order behavior. (For interpretation of the references to color in this figure legend, the reader is referred to the web version of this article.)

second-order behavior of a surface point. When the product $\kappa_1\kappa_2$, also known as the Gaussian curvature, is positive, negative, or zero, the surface is elliptic, hyperbolic, or parabolic, respectively. In the special case where κ_1 and κ_2 are equal, the surface point is umbilic. Of course, when both κ_1 and κ_2 are zero, the surface is flat. Euler's theorem tells us that the principal directions (e_1 and e_2) corresponding to the principal curvatures (κ_1 and κ_2 respectively) are mutually orthogonal. In fact, we can completely describe the second-order shape of a surface point by three intuitive parameters: the two principal curvatures, κ_1 and κ_2, and the angle ϕ made by the e_1 principal direction with an arbitrary direction in the tangent plane (Fig. 2). At an umbilic point, all normal curvatures are equal, therefore, we cannot differentiate two specific directions and associated curvatures as principal directions and principal curvatures. κ_1, κ_2, and ϕ represent exactly the same information as that in the curvature tensor, but are more accessible to novices and to visual and geometrical thinkers. We believe that this geometrical analysis results in a more intuitive and widespread understanding of second-order shape behavior.

For many geometric tasks, analysis only up to second order is not sufficient because it ignores too much shape behavior. Therefore, we need to study and understand higher-order shape behavior. We start with third-order shape analysis. We have not been able to find an intuitive description for third-order surface behavior in the differential geometry literature — all the third-order surface analysis we have seen so far uses the algebra of rank-3 tensors. As a result, a thorough understanding of third-order surface behavior is typically limited to those people who are comfortable with tensor algebra.

1.1. Contribution

In this paper, we provide an intuitive, geometric description of third-order surface behavior. Our description is similar in its intuitive nature to the readily accessible second-order description using principal curvatures and directions. We extract four shape parameters that completely describe the third-order shape behavior at a surface point. Our shape parameters are independent of any coordinate system and are obtained by decomposing the third-order shape function into its Fourier components. We also show how our approach of extracting shape parameters based on Fourier components easily generalizes to fourth- and higher-order surface analysis.

2. Previous studies of third-order surface behavior

While not as commonly studied as second-order surface behavior, third-order surface behavior has been studied for selected applications. In computer graphics, the most common application is to convey shape information via line drawings

such as suggestive contours (DeCarlo et al., 2003) or other salient features such as perceptually-based curvature extrema (Watanabe and Belyaev, 2001). Rusinkiewicz (2004) describes how the construction of the rank-3 tensor can be used to interrogate the derivatives of normal curvature in arbitrary directions. These curvature derivatives provide shape information that is perceptually important to the human visual system. While the rank-3 tensor yields precise curvature derivative information, it is not easy to understand.

In computer-aided geometric design, third-order surface energies are optimized to produce smooth surfaces. Moreton and Séquin (1992) introduced the "Minimum Variation Surface" (MVS) energy that minimizes the derivatives of principal curvatures along the respective principal directions, and Joshi and Séquin (2007) enhanced the original MVS formulation by adding cross derivative terms. Mehlum and Tarrou (1998) formulated a more complete energy by measuring inline normal curvature variation over all directions at a surface point; Gravesen and Ungstrup (2001) further enhanced the work of Mehlum and Tarrou by considering curvature variation for all surface curves (not just normal section curves). Gravesen (2004) further extended the exposition of algebra of third-order behavior by listing all the third-order invariants of a surface. Xu and Zhang (2007) minimize the variation of mean curvature of a surface by solving the corresponding (sixth-order) Euler–Lagrange equation.

Formulating such energies typically requires understanding some aspect of third-order surface behavior. For instance, Mehlum and Tarrou (1998) formulate an expression that provides the arc-length derivative of the normal curvature in a given direction. They introduce four third-order shape parameters, P, Q, S, T. These terms essentially encode the normal components of parametric surface derivatives. While useful for computing the energy values, these parameters do not easily provide a qualitative description of the third-order shape at a given point because they depend on the particular parameterization used at that point.

Third-order analysis is used to identify and characterize lines of singularities of principal curvatures on a surface. For example, Bruce et al. (1996) describe special curves called ridges (a set of points along a principal curve where the corresponding principal curvature reaches extremal values), crests (ridges where the magnitude of the extremal principal curvature is greater than that of the other principal curvature) and sub-parabolic lines (a set of points along one principal curve where the other principal curvature reaches extremal value). Sub-parabolic lines received special treatment in the paper by Morris (1997). Cazals et al. (2008) show how to calculate and approximate ridges and umbilic points on smooth surfaces. Ridges, crests and sub-parabolic lines are typically used to characterize a given surface by a sparse set of curves on that surface (see Bruce et al., 1996 for applications). However, these lines cannot be used to understand the "complete" third-order behavior of any given surface point; the analysis is restricted for special points on the surface where the principal curvature fields have singularities.

Similarly, umbilic points (surface points with equal principal curvatures) have received a lot of third-order analysis. Understanding the behavior of a surface near umbilics is useful for manufacturing thin shell parts (Maekawa et al., 1996) and studying geometrical optics (Berry and Hannay, 1977). As a result, numerous researchers have explored the exact geometric nature of umbilic points. A common method of characterizing an umbilic point is Darboux's classification according to the pattern of lines of curvature near the point (*star*, *monstar*, and *lemon* — see Berry and Hannay, 1977 for a visual description and Porteous, 2001 for a detailed description). Both Bruce et al. (1996) and Morris (1997) also provide a detailed description of the surface behavior near umbilic points in terms of ridges, crests and sub-parabolic lines. Maekawa et al. (1996) analyze the local surface geometry near an umbilic point to compute curvature lines that pass through that point. In most previous papers, the initial setup for the surface analysis near the umbilic point is similar to ours, but further analysis focuses on the umbilic classification and lacks the intuitive, qualitative description we seek.

In a nutshell, previously, researchers have extensively studied specific aspects of third-order surface behavior corresponding to particular applications, but an *intuitive, purely geometric description is missing.* Informally speaking, the "algebra of third-order behavior" has been studied sufficiently; the "geometry of third-order behavior" needs to be raised to a corresponding level of understanding. We hope that the following exposition serves as a significant step towards that goal.

3. Third-order parameters for a polynomial height field

To introduce the intuition behind the necessary mathematical concepts, we will restrict our attention to a smooth surface patch centered at a given point. Assume that the surface near the point is fully described by a third-order height field above the tangent plane at that point. The height field is a function of the two independent variables x and y such that the x–y coordinate frame forms a parameterization of the surface near the point. The height is defined by

$$z(x, y) = C_0x^3 + C_1y^3 + C_2x^2y + C_3xy^2 + Q_0x^2 + Q_1y^2 + Q_2xy + L_0x + L_1y + K. \tag{1}$$

We assume that the directions corresponding to x and y are mutually orthogonal and that the first-order (L_0, L_1) and constant parameters (K) are zero. This assumption is an over-simplification and is not always valid for a surface patch. However, we found it easier to first develop an intuition for the third-order parameters using this restricted analysis of the patch. In Section 6 we describe how to extract the third-order shape parameters for a general surface patch.

As a first step, we convert the cubic height function $z(x, y)$ into polar coordinates $z(r, \theta)$, where $r = \sqrt{x^2 + y^2}$ and $\theta = \tan^{-1}(y/x)$. We then separate the height field function (Eq. (1)) into two equations that describe only the second-order (quadratic) and third-order (cubic) behavior:

$$z_q(r,\theta) = r^2\big[Q_0\cos^2\theta + Q_1\sin^2\theta + Q_2\cos\theta\sin\theta\big], \tag{2}$$

$$z_c(r,\theta) = r^3\big[C_0\cos^3\theta + C_1\sin^3\theta + C_2\cos^2\theta\sin\theta + C_3\cos\theta\sin^2\theta\big]. \tag{3}$$

Previous work follows a similar setup up to this step. At this point, people solve for the extremal values of θ by solving the quadratic equation $\frac{\partial z_q(r,\theta)}{\partial\theta} = 0$ and cubic equation $\frac{\partial z_c(r,\theta)}{\partial\theta} = 0$ (e.g. see Mehlum and Tarrou, 1998; Maekawa et al., 1996). The roots of the quadratic equation yield the principal curvature directions. The number of real roots of the cubic equation (1) or (3) and their distribution with respect to each other is used to classify umbilic points or to study maxima of curvature variation. We have obtained a more intuitive understanding of the third-order behavior by decomposing the functions z_q and z_c into their Fourier components.

4. Fourier analysis of quadratic height function

As an introductory exercise, we analyze the Fourier components of the quadratic height function and show how the amplitudes and phase shifts of the Fourier components yield the well-known second-order shape parameters. The Fourier components of the functions that comprise $z_q(r,\theta)$ can easily be extracted:

$$\cos^2\theta = \frac{1}{2} + \frac{1}{2}\cos 2\theta, \tag{4}$$

$$\sin^2\theta = \frac{1}{2} - \frac{1}{2}\cos 2\theta, \tag{5}$$

$$\cos\theta\sin\theta = \frac{1}{2}\sin 2\theta. \tag{6}$$

Therefore, z_q can be expressed as a constant term plus a linear combination of the Fourier components $\cos 2\theta$ and $\sin 2\theta$, which can be further simplified as an equation using a single phase-shifted cosine function. That is,

$$z_q(r,\theta) = r^2\big[F_0 + F_2\cos\big(2(\theta+\phi)\big)\big], \tag{7}$$

where F_0 represents the mean value of z_q, and F_2 represents the amplitude of the cosine component that gets added to the mean. The cosine term is a symmetric function that produces four equally spaced extremal values in the range $[0, 2\pi)$. The maxima and minima correspond to the well-known principal curvatures and the mutually orthogonal principal directions. The angle ϕ is the phase shift that is measured with respect to an arbitrary, user-provided direction (usually the x-axis or the u-direction). Therefore, the entire second-order shape information can be compactly described in a parameterization-independent manner by three terms (F_0, F_2 and ϕ). Since our analysis requires an orientable surface patch, the signs of F_0 and F_2 depend on the reference normal. By computing $\kappa_1 = F_0 + F_2$ and $\kappa_2 = F_0 - F_2$ we get the three familiar terms: κ_1, κ_2, ϕ. The mean curvature is $F_0 + F_2$, while the Gaussian curvature is $F_0^2 - F_2^2$. At an umbilic point, the F_2 component is zero and ϕ can be any arbitrary angle.

5. Fourier analysis of cubic height function

Similar to the quadratic height function, we extract the Fourier components of the functions that make up $z_c(r,\theta)$:

$$\cos^3\theta = \frac{3}{4}\cos\theta + \frac{1}{4}\cos 3\theta, \tag{8}$$

$$\sin^3\theta = \frac{3}{4}\sin\theta - \frac{3}{4}\sin 3\theta, \tag{9}$$

$$\cos^2\theta\sin\theta = \frac{3}{4}\sin\theta + \frac{3}{4}\sin 3\theta, \tag{10}$$

$$\cos\theta\sin^2\theta = \frac{3}{4}\cos\theta - \frac{3}{4}\cos 3\theta. \tag{11}$$

The cubic shape function z_c can then be expressed as a linear combination of two Fourier components, $\cos\theta$ and $\cos 3\theta$ by the function

$$z_c(r,\theta) = r^3\big[F_1\cos(\theta+\alpha) + F_3\cos 3(\theta+\delta)\big], \tag{12}$$

where F_1 and F_3 are the amplitudes of the Fourier components, and α and δ are the phase shifts from the x-axis. Instead of the x-axis, we could pick an arbitrary, user-provided direction to measure the phase shifts. Similar to F_0 and F_2, the signs of F_1 and F_3 depend on the surface normal. Fig. 3 illustrates this linear combination for a fixed value of r. Fig. 4 illustrates the combination of these Fourier components to form the cubic surface.

We can consider the two phase shifts α and δ independently of each other. However, we find it more instructive to consider the direction corresponding to the (single) maximum of $F_1\cos(\theta+\alpha)$ as a "third-order principal direction". Then,

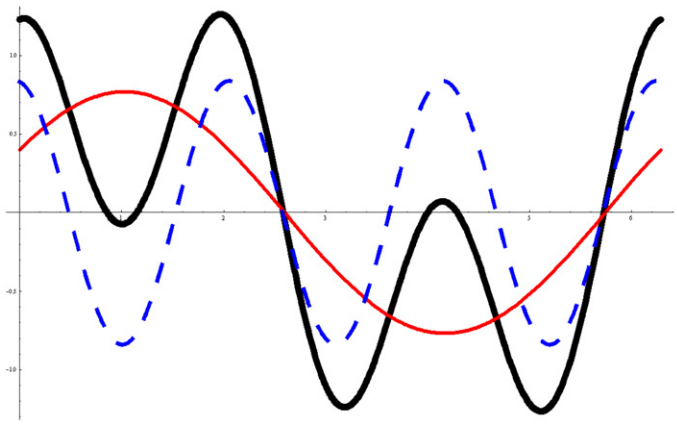

Fig. 3. Third-order height function from Eq. 3 (thick black) is a sum of two cubic sinusoidal height functions: $\cos\theta$ (solid red) and $\cos 3\theta$ (dashed blue). (For interpretation of the references to color in this figure legend, the reader is referred to the web version of this article.)

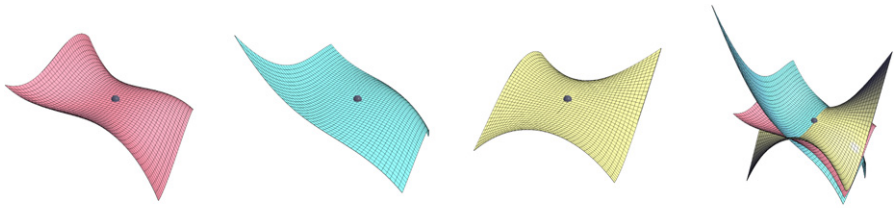

Fig. 4. The third-order surface is a combination of two sinusoidal functions ($\cos\theta$ and $\cos 3\theta$) which are the Fourier components of the third-order shape function. We show (a) the original cubic surface, (b) only the first Fourier component, (c) only the third Fourier component, and (d) the original cubic surface sandwiched between constituent Fourier components with twice their original amplitudes. Clearly, the cubic surface is the average of twice the Fourier components, $0.5(2F_1 + 2F_3)$ and therefore is equal to the sum of the Fourier components.

the phase shift δ can be expressed as $\alpha + \beta$, where β is the phase shift with respect to the third-order principal direction. Therefore, we get our final equation for describing the cubic behavior of the surface,

$$z_c(r,\theta) = r^3\big[F_1\cos(\theta+\alpha) + F_3\cos 3(\theta+\alpha+\beta)\big]. \tag{13}$$

We use the amplitudes and phase shifts of the Fourier components from Eq. (13) as our four parameterization-independent, geometrically intuitive shape parameters (illustrated in Fig. 2). These parameters can be extracted from the original third-order parameters C_0, C_1, C_2, C_3 (Eq. (3)) of the polynomial height field:

$$F_1 = \frac{\sqrt{(3C_0+C_3)^2 + (3C_1+C_2)^2}}{4}, \tag{14}$$

$$F_3 = \frac{\sqrt{(C_0-C_3)^2 + (C_2-C_1)^2}}{4}, \tag{15}$$

$$\alpha = \tan^{-1}\left(\frac{3C_1+C_2}{3C_0+C_3}\right), \tag{16}$$

$$\beta = \frac{1}{3}\tan^{-1}\left(\frac{C_2-C_1}{C_0-C_3}\right) - \alpha. \tag{17}$$

Similarly, given our third-order parameters F_1, F_3, α and β, we can extract the parameterization-dependent third-order parameters for the idealized height field above the tangent plane:

$$C_0 = F_1\cos\alpha + F_3\cos\beta, \tag{18}$$

$$C_1 = F_1\sin\alpha - F_3\sin\beta, \tag{19}$$

$$C_2 = F_1\sin\alpha + 3F_3\sin\beta, \tag{20}$$

$$C_3 = F_1\cos\alpha - 3F_3\cos\beta. \tag{21}$$

6. Computing Fourier components for a general surface patch

In this section we describe how to compute the third-order shape parameters for a point on a general surface patch. Unlike the approach taken in Section 3, we can no longer ignore the effect of lower-order shape parameters (namely, first- and second-order parameters) on the third-order shape parameters. Therefore, we cannot extract parameterization-independent shape parameters simply by analyzing a height function. Instead, we need to perform a Fourier analysis of the function that denotes the arc-length derivative of normal curvature. The Fourier coefficients can then be combined as before to yield the required shape parameters.

Consider that we have a bi-variate tensor product surface patch (e.g. a bi-cubic B-spline patch) parameterized by u, v. Given a point (u, v) in parameter space, let $\mathbf{S}(u, v)$ denote the 3D position of the point, $\mathbf{n}$ denote the unit normal, and $\mathbf{S}_u(u, v)$, $\mathbf{S}_v(u, v)$, $\mathbf{S}_{uu}(u, v)$, etc., denote the 3D parametric surface derivatives with respect to u and v. Our task is to efficiently and exactly compute the F_1, F_3, α and β parameters for any point (u, v) on the patch.

First, compute the parameterization-dependent third order shape parameters P, Q, S, and T introduced by Mehlum and Tarrou (1998):

$$P = \mathbf{S}_{uuu} \cdot \mathbf{n} + 3\mathbf{S}_{uu} \cdot \mathbf{n}_u, \tag{22}$$

$$Q = \mathbf{S}_{uuv} \cdot \mathbf{n} + 2\mathbf{S}_{uv} \cdot \mathbf{n}_u + \mathbf{S}_{uu} \cdot \mathbf{n}_v, \tag{23}$$

$$S = \mathbf{S}_{uvv} \cdot \mathbf{n} + 2\mathbf{S}_{uv} \cdot \mathbf{n}_v + \mathbf{S}_{vv} \cdot \mathbf{n}_u, \tag{24}$$

$$T = \mathbf{S}_{vvv} \cdot \mathbf{n} + 3\mathbf{S}_{vv} \cdot \mathbf{n}_v. \tag{25}$$

Then, use the formula from Mehlum and Tarrou (1998) that expresses the arc-length derivative of normal curvature as a function of the angle θ from any given reference direction

$$\begin{aligned}\kappa_n'(\theta) = \frac{1}{\sigma^3}\big[&PG^{3/2}\sin^3\theta + 3QGE^{1/2}\sin^2\theta\cos(\theta+\psi) \\ &+ 3SEG^{1/2}\sin\theta\cos^2(\theta+\psi) + TE^{3/2}\cos^3(\theta+\psi)\big],\end{aligned} \tag{26}$$

where θ is measured from the u direction, E, F and G are coefficients of the first fundamental form (the metric tensor), and $\sigma = \sqrt{F^2 - EG}$ is the area element at the point of analysis. We maintain the label $\kappa_n'(\theta)$ for the arc-length derivative of normal curvature $\kappa_n(\theta)$ as was done by Mehlum and Tarrou (1998). ψ denotes the complement to the angle between the u and v directions and is given by $\tan(\psi) = F/\sqrt{EG}$. (For the polynomial height field of Section 3, the coordinate axes were mutually orthogonal and therefore ψ was zero.)

Eq. (26) can be written as an expression similar to Eq. (3):

$$\kappa_n'(\theta) = A\cos^3(\theta+\psi) + B\sin^3\theta + C\sin\theta\cos^2(\theta+\psi) + D\sin^2\theta\cos(\theta+\psi) \tag{27}$$

where the coefficients A, B, C, and D are functions of P, Q, S, T, and E, F, and G:

$$A = \frac{TE^{3/2}}{\sigma^3}, \qquad B = \frac{PG^{3/2}}{\sigma^3}, \tag{28}$$

$$C = \frac{3SEG^{1/2}}{\sigma^3}, \qquad D = \frac{3QGE^{1/2}}{\sigma^3}. \tag{29}$$

As described in Section 5, we can perform a Fourier analysis of the sinusoidal functions in Eq. (27):

$$\cos^3(\theta+\psi) = \frac{3}{4}\cos\psi\cos\theta - \frac{3}{4}\sin\psi\sin\theta + \frac{1}{4}\cos 3\psi\cos 3\theta - \frac{1}{4}\sin 3\psi\sin 3\theta,$$

$$\sin^3\theta = \frac{3}{4}\sin\theta - \frac{1}{4}\sin 3\theta,$$

$$\cos^2(\theta+\psi)\sin\theta = -\frac{1}{4}\sin 2\psi\cos\theta - \frac{1}{4}(\cos 2\psi - 2)\sin\theta + \frac{1}{4}\sin 2\psi\cos 3\theta + \frac{1}{4}\cos 2\psi\sin 3\theta,$$

$$\cos(\theta+\psi)\sin^2\theta = \frac{1}{4}\cos\psi\cos\theta - \frac{3}{4}\sin\psi\sin\theta - \frac{1}{4}\cos\psi\cos 3\theta + \frac{1}{4}\sin\psi\sin 3\theta.$$

By grouping coefficients, we express the arc-length derivative of normal curvature as a sum of first-order and third-order sinusoidal functions

$$\kappa_n'(\theta) = F_{1\cos}\cos\theta + F_{1\sin}\sin\theta + F_{3\cos}\cos 3\theta + F_{3\sin}\sin 3\theta, \tag{30}$$

where

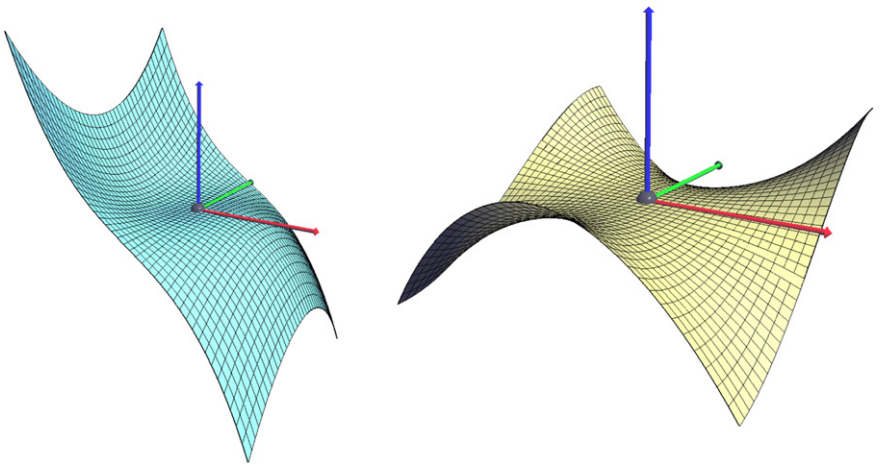

Fig. 5. The first and third Fourier components of the third-order shape function — all third-order surface behavior can be expressed as properly scaled and rotated combinations of these two shapes.

$$F_{1\cos} = \frac{1}{4}(3A\cos\psi - C\sin 2\psi + D\cos\psi), \tag{31}$$

$$F_{1\sin} = \frac{1}{4}\big(-3A\sin\psi + 3B - C(\cos 2\psi - 2) - 3D\sin\psi\big), \tag{32}$$

$$F_{3\cos} = \frac{1}{4}(A\cos 3\psi + C\sin 2\psi - D\cos\psi), \tag{33}$$

$$F_{3\sin} = \frac{1}{4}(-A\sin 3\psi - B + C\cos 2\psi + D\sin\psi). \tag{34}$$

Finally, we can combine the sine and cosine functions to formulate the arc-length derivative of normal curvature as a sum of phase-shifted sinusoidal functions of the angle θ

$$\kappa_n'(\theta) = F_1\cos(\theta+\alpha) + F_3\cos\big(3(\theta+\alpha+\beta)\big), \tag{35}$$

where the parameterization independent third-order shape parameters can be expressed in closed-form as:

$$F_1 = \frac{\sqrt{F_{1\cos}^2 + F_{1\sin}^2}}{4}, \qquad F_3 = \frac{\sqrt{F_{3\cos}^2 + F_{3\sin}^2}}{4}, \tag{36}$$

$$\alpha = \tan^{-1}\left(\frac{-F_{1\sin}}{F_{1\cos}}\right), \qquad \beta = \frac{1}{3}\tan^{-1}\left(\frac{-F_{3\sin}}{F_{3\cos}}\right) - \alpha. \tag{37}$$

To summarize, to compute the third-order shape parameters for any point u, v on a general surface patch, we need to compute the parameterization dependent third-order (P, Q, S, T) and first-order (E, F, G) parameters. Algebraic manipulation of these parameters yields the coefficients $F_{1\cos}$, $F_{1\sin}$, $F_{3\cos}$, and $F_{3\sin}$ of the four sinusoidal components of arc-length derivative of normal curvature. These four coefficients then readily yield the F_1, F_3, α and β parameters.

7. Qualitative description of the Fourier components

The shapes of the first and third Fourier components are shown in Fig. 5. Both functions are anti-symmetric with respect to π, which leads to their combination being anti-symmetric as well ($z_c(r,\theta) = -z_c(r,\pi+\theta)$) — a fact pointed out by Berry and Hannay (1977) in their study of umbilics and Mehlum and Tarrou (1998) in their study of normal curvature variation.

In the range $[0, 2\pi)$, the first Fourier component has one maximum and minimum. The shape of this component is given by the height field $z = x^3 + xy^2$ and can be understood as a lateral extrusion of the cubic curve $z = x^3$ in the y direction, enhanced by a linear component whose slope increases as the square of y (see Fig. 5). When F_1 is zero, the first Fourier component is flat and the angle α cannot be uniquely determined (in this case we set α to zero in our implementation). We consider such a point a third-order equivalent of the umbilic. Unlike the umbilic where the normal curvature is equal in all directions, at the third-order equivalent of the umbilic the normal curvature derivative does not necessarily behave the same — it is influenced by the non-zero third Fourier component. In fact, as shown by Mehlum and Tarrou (1998), the *only* situation when the normal curvature derivative is equal in all directions is when it is zero, meaning the surface is flat in third order (i.e. both F_1 and F_3 are zero).

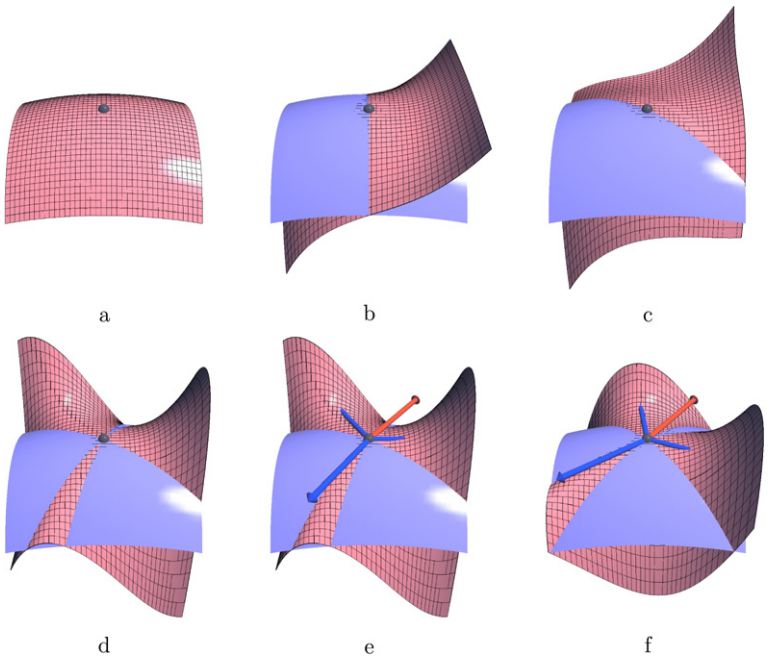

Fig. 6. *Sequence of third-order shape edits*: starting from a purely second-order surface patch where F_1 and F_3 are zero (a), we increase the amplitude F_1 of the first Fourier component (b), rotate it about the z-axis by increasing the value of α (c), and increase the amplitude F_3 of the third Fourier component (d). (e) shows the same shape as (d) but with the third-order frame indicating the directions of α and β. Finally, we rotate only the third Fourier component about the z-axis by increasing the value of β (f). The blue surface (without the grid) is the best-fitting (and unchanged) quadratic surface at the point of analysis. (For interpretation of the references to color in this figure legend, the reader is referred to the web version of this article.)

In the range $[0, 2\pi)$, the third Fourier component has three equally spaced maxima and minima. The shape of this component is similar to that of the height field $z = x^3 - 3xy^2$. This is the well-known "monkey saddle" with three peaks and troughs, each $\pi/3$ radians apart. The angle β denotes the rotation of the third Fourier component with respect to the α direction given by the first Fourier component. As shown in Fig. 6, given a fixed α and F_1, we can vary β and F_3 to change the undulatory behavior of the third order height function. When F_3 is zero, β cannot be uniquely determined. In this case, we set it to zero in our implementation.

7.1. Expressing cross derivatives using third-order shape parameters

Eq. (35) gives an expression for the *inline* derivative of curvature (κ_n') — the change of curvature is analyzed along the line for which normal curvature is measured. Alternately, we can consider *cross* derivatives of curvature ($\kappa_n^\times$), where the change of curvature is analyzed in a direction perpendicular to the line along which the normal curvature is measured. For example, functionals introduced by Gravesen and Ungstrup (2001) and Joshi and Séquin (2007) contain cross derivative terms in principal directions: $\frac{\partial \kappa_1}{\partial e_2}$ and $\frac{\partial \kappa_2}{\partial e_1}$. Here we use our third-order parameters F_1, F_3, α, and β to obtain an expression for the cross derivative of normal curvature.

Suppose we are given a surface point with normal curvature $\kappa_n(\theta)$ in a direction given by angle θ in the tangent plane. The cross derivative $\kappa_n^\times(\theta)$ is a directional derivative of $\kappa_n(\theta)$ along the direction denoted by $\theta + \pi/2$. We can show that the cross derivative is given by the formula

$$\begin{aligned}\kappa_n^\times(\theta) &= \frac{F_1}{3}\cos(\theta + \pi/2 + \alpha) - F_3 \cos 3(\theta + \pi/2 + \alpha + \beta) \\ &= -\frac{F_1}{3}\sin(\theta + \alpha) - F_3 \sin 3(\theta + \alpha + \beta). \end{aligned} \tag{38}$$

The above equation is similar to Eq. (35) which expresses the normal curvature derivative (κ_n') using the third-order shape parameters. There are three differences: (1) the F_1 component is reduced to a third of its original value, (2) the F_3 component switches sign and (3) the angles are shifted by $\pi/2$ radians.

In the rest of this section, we provide a qualitative sketch for the derivation of Eq. (38). We limit our attention to a small neighborhood around a surface point where the first fundamental form is the identity matrix and the second fundamental form is zero. A formal proof (for a general surface patch) will require a lengthy analysis similar to Section 6 and is not given here.

We can express the third-order surface information near the point of analysis by the cubic height field function used in Section 3

$$z_c(x, y) = C_0x^3 + C_1y^3 + C_2x^2y + C_3xy^2. \tag{39}$$

Suppose we are interested in the cross derivative $\kappa_{n_y}^{\times} = \frac{\partial \kappa_n(\pi/2)}{\partial x} = \frac{\partial}{\partial x}\frac{\partial^2 z_c}{\partial y^2} = \frac{\partial^3 z_c}{\partial y^2 \partial x} = 2C_3$. We will show how this cross derivative is closely related to the inline curvature derivative $\kappa'_{n_x} = \frac{\partial \kappa_n(0)}{\partial x} = \frac{\partial^3 z_c}{\partial x^3} = 6C_0$.

Consider the situation when F_1 is non-zero and F_3 is zero. Without loss of generality, we can define the x–y coordinate system around such a surface point such that $C_0 = C_3 \neq 0$ and $C_1 = C_2 = 0$ (the x-axis is along the maximal direction of the F_1 component). In this case, $\frac{\partial^3 z_c}{\partial x \partial y^2} = \frac{1}{3}\frac{\partial^3 z_c}{\partial x^3}$, which implies that the value of the cross derivative of normal curvature is equal to one third the value of the inline derivative of normal curvature, where both curvature derivatives are in the same direction. For a general direction denoted by θ, the cross derivative in the direction $\phi = \theta + \pi/2$ of the normal curvature $\kappa_n(\theta)$ is

$$\frac{\partial \kappa_n(\theta)}{\partial \mathbf{e}_\phi} = \frac{1}{3}\frac{\partial \kappa_n(\phi)}{\partial \mathbf{e}_\phi} = \frac{1}{3}F_1\cos(\phi + \alpha) = \frac{1}{3}F_1\cos(\theta + \pi/2 + \alpha) = -\frac{1}{3}F_1\sin(\theta + \alpha). \tag{40}$$

Now consider the situation when F_1 is zero and F_3 is non-zero. Without loss of generality, we can define the x–y coordinate system around such a surface point such that $C_0 = -3C_3 \neq 0$ and $C_1 = C_2 = 0$ (the x-axis is along one of the maximal directions of the F_3 component). In this case, $\frac{\partial^3 z_c}{\partial x \partial y^2} = -\frac{\partial^3 z_c}{\partial x^3}$ which implies that the value of the cross derivative of normal curvature is equal to the negative value of the inline derivative of normal curvature, where both curvature derivatives are in the same direction. For a general direction denoted by θ, the cross derivative in the direction $\phi = \theta + \pi/2$ of the normal curvature $\kappa_n(\theta)$ is

$$\frac{\partial \kappa_n(\theta)}{\partial \mathbf{e}_\phi} = -\frac{\partial \kappa_n(\phi)}{\partial \mathbf{e}_\phi} = -F_3\cos 3(\phi + \alpha + \beta) = -F_3\cos 3(\theta + \pi/2 + \alpha + \beta) = -F_3\sin 3(\theta + \alpha + \beta). \tag{41}$$

Just like the inline curvature derivative function κ'_n, we can express the cross curvature derivative function $\kappa_n^{\times}$ as a sum of its first and third Fourier components. By combining Eqs. (40) and (41), we get the expression for Eq. (38).

7.2. Expressing normal curvature derivatives in arbitrary directions using third-order shape parameters

The inline and cross derivatives are only two of the infinitely many directions in which we can compute directional derivatives of normal curvature. Given a surface point and a normal curvature $\kappa_n(\theta)$ measured along a direction given by θ, we should be able to compute the directional derivative $\frac{\partial \kappa_n(\theta)}{\partial \mathbf{e}_\psi}$ for an arbitrary direction $\mathbf{e}_\psi$. At any surface point, up to third order, we can define a rank-3 tensor that takes 3 directions as input: two (equal) directions to query the curvature tensor and specify the normal curvature and a third direction to specify the direction of normal curvature derivative (Rusinkiewicz, 2004; Gravesen and Ungstrup, 2001). We now show that the normal curvature derivatives in all directions are simple linear combinations of inline and cross curvature derivatives.

Recall the rule of directional derivatives: let f be a scalar function over a domain spanned by directions $\hat{\mathbf{x}}$ and $\hat{\mathbf{y}}$. Let the direction $\mathbf{m}$ also be spanned by the x–y basis ($\mathbf{m} = m_x\hat{\mathbf{x}} + m_y\hat{\mathbf{y}}$). Then, the directional derivative $\frac{\partial f}{\partial \mathbf{m}} = \mathbf{m} \cdot (\frac{\partial f}{\partial x}\hat{\mathbf{x}} + \frac{\partial f}{\partial y}\hat{\mathbf{y}})$.

Let the direction of the inline derivative be along the x axis, and the direction corresponding to the cross derivative be along the y axis. A vector along an arbitrary direction given by angle ψ can be written as $(\cos\psi)\hat{\mathbf{x}} + (\sin\psi)\hat{\mathbf{y}}$. Therefore, using the above rule of directional derivatives and given the inline and cross derivatives of normal curvature, $\kappa'_n(\theta)$ and $\kappa_n^{\times}(\theta)$, we can express the directional derivative of $\kappa_n(\theta)$ along the direction of ψ as:

$$\begin{aligned}\frac{\partial \kappa_n(\theta)}{\partial \mathbf{e}_\psi} &= \left((\cos\psi)\hat{\mathbf{x}} + (\sin\psi)\hat{\mathbf{y}}\right) \cdot \left(\kappa_n(\theta)'\hat{\mathbf{x}} + \kappa_n(\theta)^{\times}\hat{\mathbf{y}}\right) \\ &= \kappa'_n(\theta)\cos\psi + \kappa_n^{\times}(\theta)\sin\psi \end{aligned} \tag{42}$$

where ψ is computed as the offset angle from the direction of θ.

Eq. (42) is significant because it shows that at a surface point, the derivative of any normal curvature in any direction can be expressed as a function of the F_1, F_3, α and β parameters. This is another way of observing that the F_1, F_3, α and β parameters fully describe the third-order shape of a surface point.

8. Applications

We present two applications from geometric analysis and design that benefit from having an intuitive understanding of third-order shape.

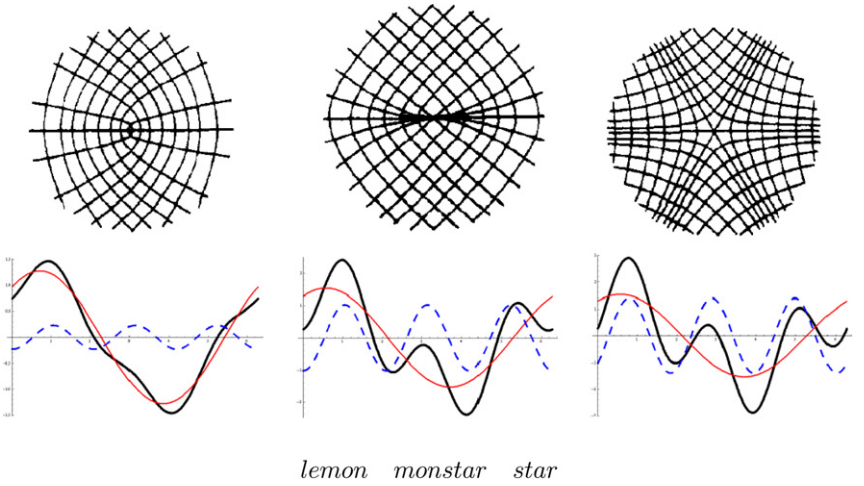

Fig. 7. Principal curvature lines near the three types of umbilic points with the graphs of corresponding third-order height functions (thick black). The top row of figures is from Berry and Hannay (1977). The number of extrema (two or six) and zero crossings (two or six) of the height function together determine the type of the generic umbilic point. Notice how the first Fourier component (solid red) dominates the overall third-order behavior for the *lemon* umbilic, while the third Fourier component (dotted blue) creates local extrema in the *monstar* umbilic and additional zero crossings of the height function in the *star* umbilic. (For interpretation of the references to color in this figure legend, the reader is referred to the web version of this article.)

8.1. Classification of umbilics

As the first example, we show how to use our third-order shape parameters to understand the surface behavior near umbilic points (points with equal principal curvatures). As mentioned before, generic umbilic points on surfaces are classified according to the pattern made by lines of curvature as they pass through the point. Since the surface behavior up to second order is uniform in all directions, we need a third-order analysis to classify umbilics. As presented by Berry and Hannay (1977), based on the pattern of lines of principal curvature near the point, there are three types of generic (stable) surface umbilics: *lemon*, *monstar* and *star* (see Fig. 7). The pattern of lines of principal curvature depends on the number of real, distinct roots of the cubic equations $z_c(r,\theta) = 0$ (z_c from Section 3) and $\frac{\partial z_c(r,\theta)}{\partial \theta} = 0$. The roots can be obtained by computing the discriminants of the two cubic equations (the third-order height function and $\frac{\partial z_c(r,\theta)}{\partial \theta} = 0$). Porteous (2001) presents a more accessible method using complex analysis that is often used in practice.

Our third-order shape parameters offer an alternative, visual and high-level explanation of when different types of umbilics are formed. When the first Fourier component dominates the overall third-order behavior, we get only one maximum and minimum for $z_c(r,\theta)$. In that case, we have the *lemon* type of umbilic. When the third Fourier component is strong enough that its derivatives (slope) exceed those of the first component, we get three distinct maxima and minima (six real roots for the equation $\frac{\partial z_c(r,\theta)}{\partial \theta} = 0$) and obtain the *monstar* umbilic. If the third Fourier component dominates the third-order height function and creates six zero crossings (instead of two), we get the *star* type of umbilic. Fig. 7 compares the network of curvature lines to the number of zeros and extrema of the third-order height function evaluated along a small circle around the umbilic point.

8.2. Constructing surface design functionals

In a recently published thesis (Joshi, October 2008), we used the third-order shape parameters F_1, F_3, α and β to formulate surface energy functionals that produce aesthetically pleasing shapes upon minimization. We showed that the functional introduced by Mehlum and Tarrou (1998) is a "complete" third-order functional because it measures all the curvature-derivative information at a surface point, and is conveniently given by the sum of the squares of the F_1 and F_3 terms.

Mehlum and Tarrou (1998) argue that to measure the total curvature variation at a surface point, one should compute the average of the squared magnitude of the arc-length derivative of normal curvature across all directions.

$$\text{Mehlum–Tarrou energy} = \frac{1}{\pi}\int\left(\int_0^{\pi} \kappa_n'(\theta)^2\, d\theta\right) dA \tag{43}$$

where $\kappa_n'(\theta)$ is a directional derivative of $\kappa_n(\theta)$ in the direction denoted by angle θ in the tangent plane. The Mehlum–Tarrou energy was introduced with a complicated closed-form expression (Eq. (34) in Mehlum and Tarrou, 1998), but can be simply expressed by using our third-order shape parameters. In particular, we show that the Mehlum–Tarrou energy is the sum of squares of the amplitudes of the two Fourier components that define third-order surface behavior.

Fig. 8. Different optimal shapes obtained by minimizing (a) the F_1^2 energy, (b) the F_3^2 energy, and (c) their sum (which corresponds to the Mehlum–Tarrou energy). For a detailed description of this and other examples, please refer to Joshi (October 2008).

$$\begin{aligned}
&\text{Mehlum–Tarrou energy}\\
&= \frac{1}{\pi}\int\left(\int_0^{\pi} \kappa_n'(\theta)^2\,d\theta\right)dA\\
&= \frac{1}{\pi}\int\left(\int_0^{\pi} \big(F_1\cos(\theta+\alpha)+F_3\cos 3(\theta+\alpha+\beta)\big)^2\,d\theta\right)dA\\
&= \frac{1}{2}\int F_1^2+F_3^2\,dA. \qquad (44)
\end{aligned}$$

In the above derivation, we use the orthogonality of the cosine function: $\int_0^{\pi}\cos(\theta+\gamma)\cos 3(\theta+\delta)\,d\theta = 0$ for any constants γ and δ. Thus, the Mehlum–Tarrou energy is independent of the phase shift β of the third Fourier component.

While the total computational cost necessary to compute F_1 and F_3 may not be smaller than that of the expression given by Mehlum and Tarrou (Eq. (34) of Mehlum and Tarrou, 1998), we believe our Fourier components allow us to provide a simpler, more intuitive explanation of their third-order energy.

We can modify Eq. (44) to obtain a weighted form of the SI-Mehlum–Tarrou energy, where the weights are used to favor or ignore the first or third Fourier components of the curvature derivative function,

$$\text{weighted Mehlum–Tarrou energy} = \frac{1}{2}\int w_1F_1^2 + w_3F_3^2\,dA. \qquad (45)$$

Similarly, we can obtain an energy functional that measures the amplitude of only one of the two components of the curvature derivative function:

$$F_1^2 \text{ energy} = \int F_1^2\,dA, \qquad (46)$$

$$F_3^2 \text{ energy} = \int F_3^2\,dA. \qquad (47)$$

In the thesis (Joshi, October 2008) we showed that all surface energies consisting of only third-order terms can be expressed as combinations of the F_1 and F_3 terms. Therefore, the F_1 and F_3 terms are useful for constructing a basis that spans the range of all third-order functionals. In Fig. 8 we show a comparison of the different types of shapes preferred by the third-order basis functionals.

9. Higher order surface analysis

So far we have concentrated on extracting the parameters that intuitively describe third-order surface behavior. In this section we will show how our approach based on Fourier analysis of the shape function easily extends to arbitrary orders. Similar to the method from Section 5 the Fourier components of the fourth-order height function are $r^4\cos 0$, $r^4\cos 2\theta$ and $r^4\cos 4\theta$. Therefore, the five parameterization-independent, intuitive parameters that fully describe fourth-order shape are the amplitudes and phase shifts of the $\cos 0$, $\cos 2\theta$ and $\cos 4\theta$ functions (the $\cos 0$ function has constant amplitude and thus no phase shift). Similarly, the six parameters that intuitively describe fifth-order shape are the amplitudes and phase shifts of the $\cos\theta$, $\cos 3\theta$ and $\cos 5\theta$ functions. See Fig. 9 for an illustration of these basis shapes.

In general, $n+1$ parameters are sufficient for fully and intuitively describing the nth-order shape of a surface point. The parameters are the amplitudes and phase shifts associated with the Fourier components of the shape function. If n is even, the Fourier components are $r^n\cos(kt)$ where $k = 0, 2, 4, \ldots, n$. In this case, the nth-order shape function consists of $\frac{n}{2}$

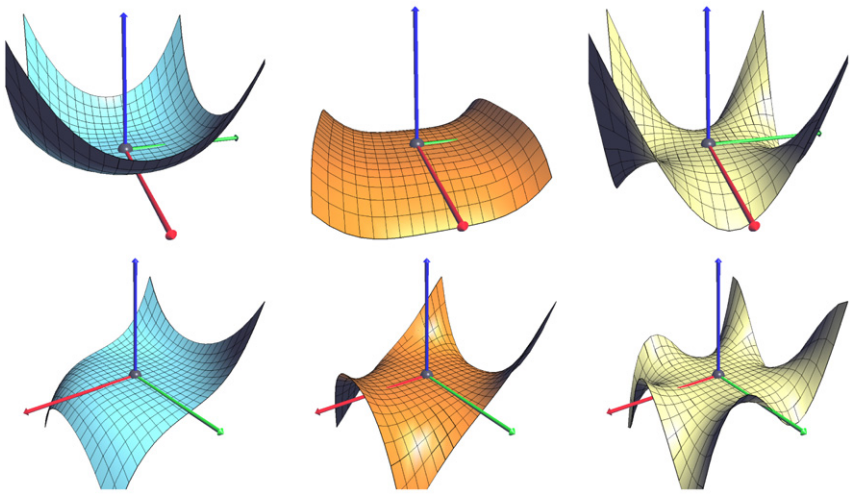

Fig. 9. The first row shows the three Fourier components of the fourth-order shape function — all fourth-order surface behavior can be expressed as properly scaled and rotated combinations of these three shapes. Similarly, the second row shows the three Fourier components of the fifth-order shape function.

phase shifts and $\frac{n}{2}+1$ amplitudes. If n is odd, the Fourier components are $r^n\cos(lt)$ where $l = 1, 3, 5, \ldots, n$. In this case, the nth-order shape function consists of $\frac{n+1}{2}$ phase shifts and $\frac{n+1}{2}$ amplitudes.

10. Summary

We have presented an intuitive analysis of third- and higher-order surface behavior in terms of the Fourier components of the appropriate shape function. We hope our exposition will be useful as a tool for studying and characterizing higher-order geometric terms of surface behavior for modeling and optimization purposes.

References

Berry, M., Hannay, J., 1977. Umbilic points on Gaussian random surfaces. Journal of Physics A: Mathematical and General 10 (11), 1809–1821. URL http://stacks.iop.org/0305-4470/10/1809.

Bruce, J., Giblin, P., Tari, F., 1996. Ridges, crests and sub-parabolic lines of evolving surfaces. International Journal of Computer Vision 18 (3), 195–210.

Cazals, F., Faugere, J.-C., Pouget, M., Rouillier, F., 2008. Ridges and umbilics of polynomial parametric surfaces. In: Geometric Modeling and Algebraic Geometry. Springer-Verlag, Berlin, pp. 141–159.

DeCarlo, D., Finkelstein, A., Rusinkiewicz, S., Santella, A., 2003. Suggestive contours for conveying shape. ACM Transactions on Graphics 22 (3), 848–855.

Gravesen, J., Ungstrup, M., 2001. Constructing invariant fairness measures for surfaces. Advances in Computational Mathematics 17 (1), 67–88.

Gravesen, J., 2004. Third order invariants on surfaces. In: Computational Methods for Algebraic Spline Surfaces. Springer-Verlag, Berlin, pp. 67–88.

Joshi, P., October 2008. Minimizing curvature variation for aesthetic surface design. Ph.D. thesis, EECS Department, University of California, Berkeley. URL http://www.eecs.berkeley.edu/Pubs/TechRpts/2008/EECS-20.

Joshi, P., Séquin, C., 2007. Energy minimizers for curvature-based surface functionals. Computer-Aided Design and Applications 4 (5), 607–617.

Maekawa, T., Wolter, F., Patrikalakis, N., 1996. Umbilics and lines of curvature for shape interrogation. Computer-Aided Geometric Design 13 (2), 133–161.

Mehlum, E., Tarrou, C., 1998. Invariant smoothness measures for surfaces. Advances in Computational Mathematics 8 (1), 49–63.

Moreton, H., Séquin, C., 1992. Functional optimization for fair surface design. In: SIGGRAPH, pp. 167–176.

Morris, R., 1997. The sub-parabolic lines of a surface. In: IMA Conference on the Mathematics of Surfaces, pp. 79–102.

Porteous, I., 2001. Geometric Differentiation, 2nd edition. Cambridge University Press.

Rusinkiewicz, S., 2004. Estimating curvatures and their derivatives on triangle meshes. In: Symposium on 3D Data Processing, Visualization, and Transmission.

Watanabe, K., Belyaev, A., 2001. Detection of salient curvature features on polygonal surfaces. Computer Graphics Forum 20 (3).

Xu, G., Zhang, Q., 2007. G2 surface modeling using minimal mean-curvature-variation flow. Computer-Aided Design 39 (5), 342–351.